Macromolecular Research, Vol. 17, No. 5, pp 307-312 (2009)

Relative Parameter Contributions for Encapsulating Silica-Gold Nanoshells by Poly(*N*-isopropylacrylamide-*co*-acrylic acid) Hydrogels

Min-Yim Park, Sera Lim, and Sang-Wha Lee*

Department of Chemical & Bio Engineering, Kyungwon University, Gyeonggi-do 461-701, Korea

Sang-Eun Park

Advanced Energy Materials Processing Laboratory, Korea Institute of Science and Technology, Seoul 130-650, Korea

Received February 7, 2008; Revised January 16, 2009; Accepted January 16, 2009

Abstract: Core-shell hydrogel nanocomposite was fabricated by encapsulating a silica-gold nanoshell (SGNS) with poly(*N*-isopropylacrylamide-*co*-acrylic acid) (PNIPAM-*co*-AAc) copolymer. The oleylamine-functionalized SGNS was used as a nanotemplate for the shell-layer growth of hydrogel copolymer. APS (ammonium persulfate) was used as a polymerization initiator to produce a hydrogel-encapsulated SGNS (H-SGNS). The amounts of NIPAM (*N*-isopropylacrylamide) monomers were optimized to reproduce the hydrogel-encapsulated SGNS. The shell-layer thickness was increased with the increase of polymerization time and no further increase in the shell-layer thickness was clearly observed over 16 h. H-SGNS exhibited the systematic changes of particle size corresponding to the variation of pH and temperature, which was originated from hydrogen-bonding interaction between PNIPAM amide groups and water, as well as electrostatic forces attributed by the ionization of carboxylic groups in acrylic acid.

Keywords: gold nanoshell, hydrogel, poly(*N*-isopropylacrylamide), plasmon resonance.

Introduction

Hydrogel-based materials are actively developed for biomedical applications owing to their biocompatibility and large hold-up of soluble materials.[1-3] They usually undergo discontinuous volume changes according to the variation of physico-chemical factors such as pH, temperature, light, and electromagnetic field.[4-6] Poly(*N*-isopropylacrylamide) (PNIPAM) and its copolymer are intensively investigated in drug delivery system because of their nontoxicity and remarkable thermosensitivity.[7,8] Homo-polymer NIPAM hydrogels, however, are limited in the application to a biological system because thermally-induced volume changes occur at a fixed LCST of 32-33 °C that is lower than body temperature.[9] This limitation can be circumvented by incorporating acrylic acid (AAc) or acrylamide (AAm) moieties into the polymer backbone, which can shift the LCST of the PNIPAM hydrogel in the range of 35-60 °C by adjusting the relative amounts of AAc (or AAm) to NIPAM components.[10] Furthermore, poly(*N*-isopropylacrylamide-*co*-acrylic acid) copolymer exhibits a reversible swelling-deswelling transition in response to the systematic variation of pH and temperature.[11]

*Corresponding Author. E-mail: lswha@kyungwon.ac.kr

Gold nanoparticles are attractive components in optically-responsive biomaterials owing to their non-cytotoxicity and unique optical properties. A silica-gold nanoshell that consists of a dielectric silica core surrounded by a thin gold layer can demonstrate a hyperthermia effect via plasmon-derived strong absorption of NIR light (800-1,200 nm) that can effectively penetrate human tissue and bone.[12,13] Recently, gold-hydrogel nanostructures have been investigated as a potential candidate to molecular electronics, biosensors, and drug delivery devices[3,14,15] If thermally-sensitive materials are coated on the silica-gold nanoshells (SGNSs), this new hybrid nanostructure can play as a smart drug-delivery system which can be activated by NIR light irradiation.

Here, we described a synthetic route for the encapsulation of a silica-gold nanoshell (SGNS) with a shell-layer of poly (*N*-isopropylamide-*co*-acrylic acid) copolymer: i) preparation of oleylamine-functionalized SGNS, ii) encapsulation of SGNS core with hydrogel shell. In particular, the relative contributions of experimental parameters in the fabrication of hydrogel-encapsulated SGNSs (H-SGNSs) were systematically investigated, such as NIPAM concentration, and polymerization time at constant temperature. The size changes of H-SGNSs corresponding to the variation of pH and temperature were analyzed by dynamic light scattering (DLS).

Experimental

Chemical Materials. All the reagents were used as a received form from Aldrich Chemical Co.: 3-aminopropyl trimethoxysilane (APTMS, 97%), tetraethyl orthosilicate (TEOS, 99.999%), tetrakis (hydroxymethyl) phosphonium chloride (THPC, 80% solution in water), ammonium hydroxide (NH_4OH, 28% NH_3 in water), formaldehyde (HCHO, 37 wt%), hydrogen tetrachloroaurate (III) hydrate ($HAuCl_4$, 99.9+%), potassium carbonate (K_2CO_3, 99.7%), absolute ethanol (C_2H_5OH, 99.5%), sodium hydroxide (NaOH, semiconductor grade), *N*-isopropylacrylamide (NIPAM), acrylic acid (AAc), cross-linker *N,N*-methylenebisacrylamide (BIS, 99%), ammonium persulfate (APS), and oleylamine (Tech. 70%).

Silica-Gold Nanoshells (SGNSs). Silica nanoparticles were prepared at 48 °C by the Stöber method. 3.9 mL Ammonium (28% NH_3 in water) and 1.5 mL TEOS was added into 45 mL ethanol solution and stirred overnight. The condensation of tetraethyl orthosilicate generally started within 10 min, which was easily observed through the color change from colorless to opaque.[16] To prepare gold seeds of 1-3 nm, 0.5 mL of 1.0 M NaOH and THPC (1.0 mL of 50 mmol/L aqueous solution) were mixed with 45 mL of HPLC grade water, and 2.0 mL of 1.0 wt% tetrachloroaurate (III) trihydrate was added quickly and stirred vigorously for 5 min.[17]

An excess of APTMS was added to the colloidal silica solution with vigorous stirring for 2 h. To enhance the covalent bonding of APTMS groups on the silica surface, the solution was gently heated at 70 °C for 1 h. And then, 0.5 mL of APTMS-functionalized silica nanoparticles were mixed with gold seeds to obtain gold-deposited silica nanoparticles.[18] The seed-mediated growth of gold layer over silica cores was carried out in the presence of gold salts (K^+AuCl_4) and a reducing agent (formaldehyde).

Hydrogel-Encapsulated Silica-Gold Nanoshells (H-SGNSs). Silica-gold nanoshell solution was diluted with purified HPLC grade water and transferred to a three-necked round-bottomed flask equipped with a reflux condenser and an inlet for nitrogen gas. An aliquot (3.2 mL of 0.001 M solution) of oleylamine was added and stirred for 1 h to functionalize the surface of SGNS. Oleylamine-functionalized SGNSs (O-SGNSs) were separated by centrifugation for 20 min at 10,000 rpm and the purified nanoparticles were diluted with HPLC grade water.

An approximately 94:6 wt% ratio of NIPAM (26.1 mL of 0.01 M solution) to AAc (1.6 mL of 0.01 M solution) was then added into the solution containing O-SGNSs and cross-linker BIS (1.3 mL of 0.01 M solution). The solution was heated to 70 °C, and then APS (0.8 mL of 0.01 M solution)

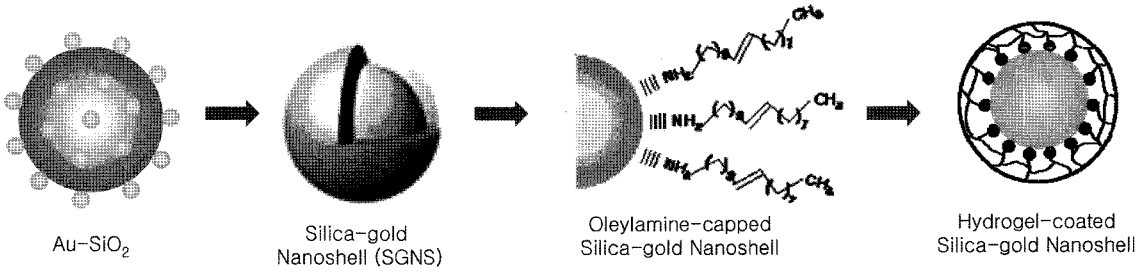

(a)

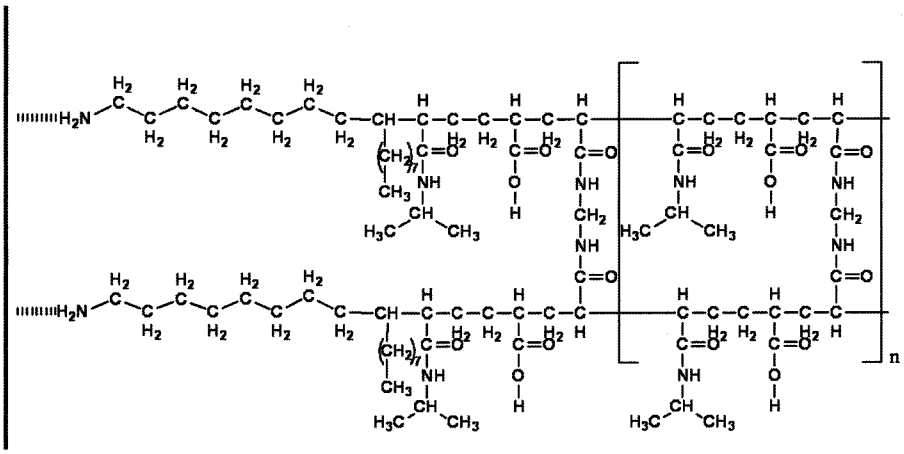

(b)

Figure 1. (a) Schematic illustration for the fabrication of hydrogel-encapsulated silica-gold nanoshells (H-SGNSs)[6,11] and (b) The proposed chemical structure of encapsulated poly(*N*-isopropylacrylamide-*co*-acrylic acid) copolymer.

was added to initiate the polymerization reaction with constant stirring for predetermined reaction time (4-16 h).[11] Nitrogen gas was continuously bubbled throughout the polymerization process to remove the residual oxygen, which can intercept radicals and/or disrupt the polymerization reaction. The final products were separated by centrifugation for 20 min at 10,000 rpm, and the supernatant was carefully discarded to eliminate any unreacted materials and oligomers. The hydrogel-encapsulated SGNSs (H-SGNSs) diluted with HPLC grade water was filtered through a filter paper to remove large impurities and microgels and stored at room temperature for the subsequent characterization. Figures 1(a) and (b) summarized the whole fabrication process of H-SGNSs and the proposed chemical structure of the encapsulated shell-layer consisting of poly(*N*-isopropylacrylamide-*co*-acrylic acid) copolymer (MIPAM: acrylic acid= 96: 4 vol%) with some moieties of APS initiator, BIS cross-linker, and oleylamine ligand.

Characterization Instruments. UV-Vis optical spectrometer (wavelength 200-1,100 nm) was used to investigate the optical properties of silica-gold nanoshells. Surface morphology of nanoparticles was analyzed by FE-SEM (Hitachi S-4700) operating at 15 kV. Dynamic light scattering (DLS) was used to measure pH-sensitive and thermo-responsive changes of particle size through frequency change (or shift) information of scattering light. DLS instrument (Bl-9000AT/ 200SM, USA) was controlled precisely by circulating the water outside the sample chamber. FIB (Focused Ion Beam) operating at 30 keV was used for a cross-sectional view of H-SGNS that was generated by FIB milled trenches. Then, Pt metal line is deposited on the area of interest to prevent damage and spurious sputtering of the top portion of the specimen.[19]

Results and Discussion

Oleylamine-Functionalized Silica-Gold Nanoshells (O-SGNSs). The silica nanoparticles of ca. 160 nm diameter were prepared by the well-known Stöber method, and gold seeds of 1-3 nm were prepared by THPC/NaOH reduction method. Figure 2 compared the UV-Vis spectra of silica nanoparticles, gold seeds, Au-deposited SiO_2, and silica-gold nanoshells. The plasmon-derived absorption peak of gold-deposited silica nanoparticles almost coincided with that of gold colloids, indicating the monodisperse deposition of gold seeds on the surface of silica nanoparticles. The surface plasmon resonance of thin gold layer over dielectric silica cores induced the red-shift of absorption peak into NIR region of 750-850 nm. The gold layer thickness was estimated as ca. 30 nm (core/shell ratio=5) according to the SEM images.

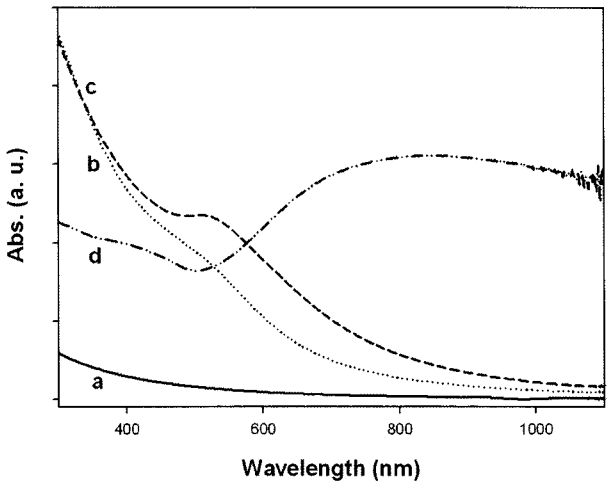

Figure 2. UV-Vis spectra of nanoparticles: (a) silica colloids, (b) gold seeds, (c) gold-deposited silica nanoparticles (Au-SiO_2), (d) silica-gold nanoshells (SGNSs).

The surface of SGNS was self-assembled by oleylamine ligand having terminal hydrophobic carbon chains. Oleylamine-functionalized SGNSs (O-SGNSs) were dispersed in various medium solvents (such as water, ethanol, and toluene). The surface plasmon resonance was affected by several factors such as core-shell ratio, nanoshell geometry, dielectric constant of core material, and refractive index of medium solvent.[20] As seen from Figure 3, the plasmon-derived absorption peaks of O-SGNSs were more red-shifted with

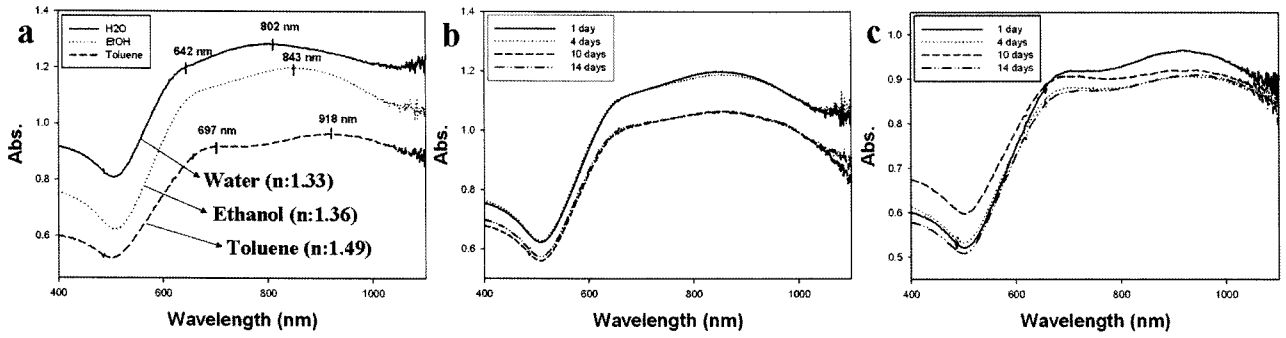

Figure 3. UV-Vis spectra of oleylamine-functionalized silica-gold nanoshells (O-SGNSs) dispersed in (a) various solvents with different storage times in (b) ethanol and (c) toluene.

the increase of refractive index of medium solvent.[21]

The UV-Vis spectra of O-SGNSs were also investigated with the elapse of storage times in various medium solvents. The polarity of medium solvents are decreased in the following order: Water (10.2) > Ethanol (5.2) > Toluene (2.4). As shown in Figures 3(b) and (c), the O-SGNSs in ethanol with relatively high polarity exhibited a fair decrease of absorption intensity after one week of storage times, whereas the O-SGNSs in toluene with low polarity maintained the almost constant absorption peak even for two weeks of storage times. The O-SGNSs with hydrophobic carbon chains exhibited a slight aggregation of colloidal particles in ethanol solvent, whereas toluene solvent gave more enhanced colloidal stability of O-SGNSs due to a favorable hydrophobic-hydrophobic interaction. Moreover, the distinct split of plasmon-derived absorption peaks was observed owing to the enhanced dispersion of O-SGNSs in toluene (see Figure 3(a)).

Hydrogel-Encapsulated Silica-Gold Nanoshells (H-SGNSs). The polymerization of N-isopropyl acrylamide (NIPAM) was initiated by the addition of persulfate initiators and cross-linking agents at 70 °C.[22] Polymerized NIPAM chains are stabilized by charge groups originating from an ionic initiator (or ionic surfactant).[23] Water-soluble ammonium persulfates (APS) was used as a radical initiator for NIPAM polymerization at 70 °C.

NIPAM monomer was diluted to find the optimal concentration in the fabrication of H-SGNSs. NIPAM concentration higher than 0.01 M (0.026 mmol in 26.1 mL solution) produced not only very thick hydrogel-shell over SGNS but also microgel composites embedded by SGNSs, as shown in Figures 4(a) and (b). If the concentration of NIPAM was decreased by 1/50~1/100 of 0.026 mmol, H-SGNSs were successfully produced without distinct observation of large microgel composites, as shown in Figures 4(c) and (d). The ratio of $\Delta\lambda$(H-SGNS)/$\Delta\lambda$(SGNS) was decreased with the increase of NIPAM concentration, indicating the increase of shell-layer thickness over the surface of SGNS. In summary, the optimal amounts of NIPAM were determined as 1/50~1/100 of 0.01 M of NIPAM concentration, which reproduced H-SGNS with a well-defined surface morphology and discrete size distribution. However, a very low concentration of NIPAM rather produced an incomplete coverage of hydrogel-shell over the surface of SGNS.

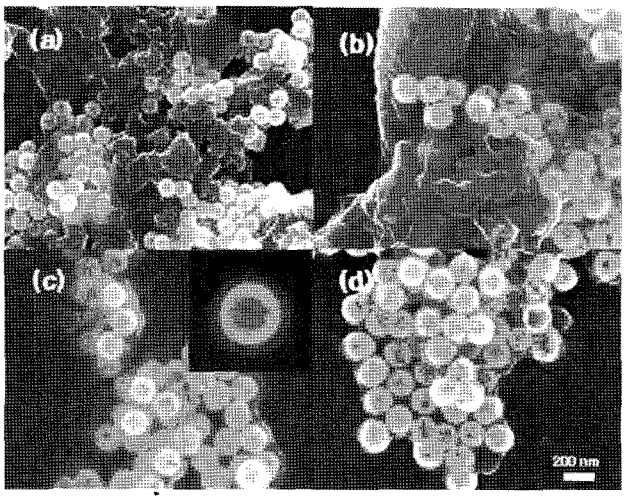

Figure 4. SEM images of hydrogel-encapsulated silica-gold nanoshells (H-SGNSs) at different NIPAM amounts in aqueous solution of 26.1 mL: (a) 0.13 mmol, (b) 0.026 mmol, (c) 5.22×10^{-3} mmol, and (d) 2.61×10^{-3} mmol.

Table I. The Size and Optical Properties of Hydrogel-Encapsulated Silica-Gold Nanoshells (H-SGNSs) with the Increase of Reaction Times

Reaction Time(h)		0	4	12	16
H-SGNS	Size(nm)	212.8	243.6	252.9	318.7
	$\Delta\lambda_1/\Delta\lambda_2$	1.00	0.55	0.25	0.07
	λ_{max}(nm)	773	757	751	619

*$\Delta\lambda$ indicate the depth difference of minimal and maximal heights of absorption peaks.
**The original solution of H-SGNSs exhibited acidic range of pH 4.9.

At the optimized concentration of NIPAM, APS-initiated shell-layer formation was investigated with the increase of polymerization times (see Table I). With the increase of reaction time, the thickness of hydrogel shell-layer was increased from ca. 20 nm at 4 h to ca. 50 nm at 16 h. FIB images also confirmed that the shell-layer thickness was increased at longer polymerization time (see Figure 5). After 16 h, further increase of hydrogel-shell thickness was not clearly observed. As seen in Table I, the UV-Vis spectra of H-SGNSs were blue-shifted and broadened with the increase of shell-layer thickness. Walt and his coworker showed that plasmon-derived absorption bands of PMMA-coated gold nanoparticles were blue-shifted when the polymer was directly coated on the surface of gold nanoparticles.[24] The hydrogel shell-layer may interfere with the plasmonic vibration of SGNS and a consequent diminishment of surface plasmon resonance.

Under the optimized conditions and 14 h of polymerization time, H-SGNSs were prepared to investigate the characteristic pH-sensitive and thermo-responsive behaviors of hydrogel nanocomposites. According to the measurements of dynamic light scattering (DLS), H-SGNSs did not exhibit a clear indication of the aggregated H-SGNSs and/or multiple SGNSs encapsulated by hydrogels at pH5 of original solution (data not shown). The average particle size of H-SGNSs was increased by ca. 100 nm with the increase of solution pH (from pH5 to pH7).[4,6] The increase of particle size was attributed to the encapsulated-hydrogel layer expansion caused by the electrostatic repulsion of carboxylic groups in AAc.

As shown in Figure 6, H-SGNSs exhibited the reversible variation of particle size in response to the changes of pH

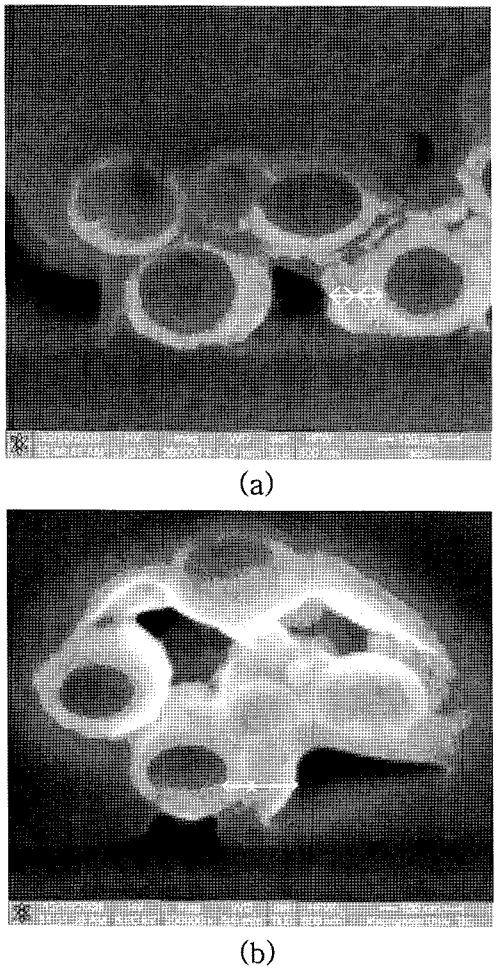

Figure 5. FIB images of hydrogel-encapsulated silica-gold nanoshells (H-SGNSs) at different polymerization times: (a) 4 h and (b) 16 h.

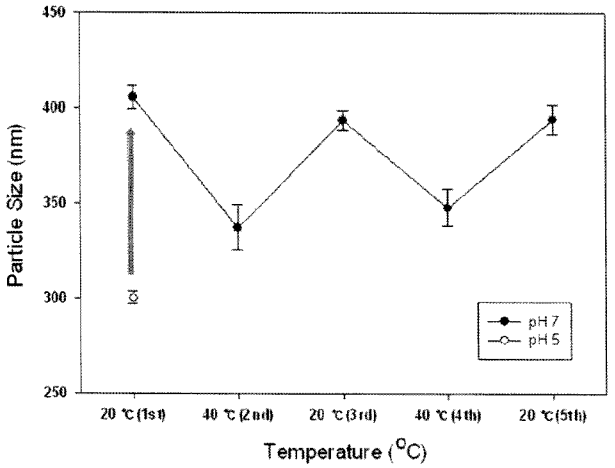

Figure 6. The size variation of hydrogel-encapsulated silica-gold nanoshells (H-SGNSs) in response to the alteration of pH and temperature.

and temperature. The H-SGNSs exhibited the systematic alteration of particle size as a function of temperature, i.e.,

Table II. Statistical Analysis of H-SGNS Size Corresponding to the pH and Temperature Changes

	20 °C	40 °C	20 °C	40 °C	20 °C
pH5	300.2 ±3.1 nm				
pH7	405.5 ±6.1 nm	337.3 ±12 nm	393.6 ±5.1 nm	347.9 ±9.6 nm	393.9 ±7.5 nm

*The particle size was measured three times for each sample.

repeated cycles of cooling and heating showed the variation of average particle size within 2.2% deviation. The collapse of NIPAM hydrogels above LCST occurred by the breakage of hydrogen bonding between NIPAM amide groups and water, along with the simultaneous increase of internal interactions of the hydrogel matrix.[3,6] Table II showed the statistical analysis for the respective particle size corresponding to pH changes from pH5 to pH7 and temperature changes from 20 to 40 °C, respectively.

Conclusions

Oleylamine-functionalized silica-gold nanoshells (O-SGNSs) exhibited enhanced colloidal stability in toluene because the surface of O-SGNSs was covered by long hydrocarbon chains with hydrophobicity. As a single initiator of APS, SGNSs were successfully encapsulated by hydrogel shell-layer of PNIPAM-*co*-AAc copolymers. The NIPAM concentration was optimized as 1/50~1/100 of 0.01 M (0.26 mmol in 26.1 mL solution) for the reproduction of hydrogel-encapsulated SGNSs (H-SGNSs). The optical ratio of $\Delta\lambda$ (H-SGNS)/$\Delta\lambda$(SGNS) was decreased with the increase of polymerization time, owing to the increase of shell-layer thickness over the surface of SGNS. The hydrogel-encapsulated SGNSs exhibited the reversible variation of particle size in response to the pH and temperature changes.

Acknowledgments. This work was supported by the GRRC program of Gyeonggi province (GRRC) [2008-0171].

References

(1) R. M. K. Ramanan, P. Chellamuthu, L. Tang, and K. T. Nguyen, *Biotechnol. Prog.*, **22**, 118 (2006).
(2) J. W. Lee, D. S. Lee, and S. W. Kim, *Macromol. Res.*, **11**, 189 (2003).
(3) Y. Qui and K. Park, *Adv. Drug Deliver. Rev.*, **53**, 321 (2001).
(4) A. M. Atta, N. E. Maysour, and K. E. Arndt, *J. Polym. Res.*, **13**, 53 (2006).
(5) J. Ma, Y. Xu, Q. Zhang, L. Zha, and B. Liang, *Colloid Polym. Sci.*, **285**, 479 (2007).
(6) J. H Kim and T. R. Lee, *Polym. Mater. Sci. Eng.*, **90**, 637 (2004).
(7) Y. Hirokawa and T. Tanaka, *J. Chem. Phys.*, **81**, 6379 (1984).
(8) J. W. Lee, D. S. Lee, and S. W. Kim, *Macromol. Res.*, **11**, 189

(2003).
(9) H. G. Schild, *Prog. Polym. Sci.*, **17**, 163 (1992).
(10) M. J. Snowden, B. Z. Chowdhry, B. Vincent, and G. E. Morris, *J. Chem. Soc. Faraday Trans.*, **92**, 5013 (1996).
(11) J.-H. Kim and T. R. Lee, *Drug Dev. Res.*, **67**, 61 (2006).
(12) Y. Sun and Y. Xia, *Anal. Chem.*, **74**, 5297 (2002).
(13) T. Pham, J. B. Jackson, N. J. Halas, and T. R. Lee, *Langmuir*, **18**, 4915 (2002).
(14) S. R. Sershen, G. A. Mensing, N. J. Halas, D. J. Beebe, and J. L. West, *Adv. Mater.*, **17**, 1366 (2005).
(15) X. Zhao, X.-Ding, Z. Deng, Z. Zheng, Y. Peng, and X. Long, *Macromol. Rapid. Commun.*, **26**, 1784 (2005).
(16) W. Stöber and A. Fink, *J. Colloid Interf. Sci.*, **26**, 62 (1968).
(17) S. Park, M. Park, P. Han, and S. Lee, *J. Ind. Eng. Chem.*, **13**, 65 (2007).
(18) S.-E. Park, M.-Y. Park, P.-K. Han, and S.-W. Lee, *Bull. Korean Chem. Soc.*, **27**, 1341 (2006).
(19) L. A. Giannuzzi and F. A. Steve, *Micron*, **30**, 197 (1999).
(20) S. L. Westcott, S. J. Oldenberg, T. R. Lee, and N. J. Halas, *Langmuir*, **14**, 5396 (1998).
(21) F. Tam and N. Halas, *Progress in Organic Coatings*, **47**, 275 (2003).
(22) B. R. Saunders and B. Vincent, *Adv. Colloid Interf. Sci.*, **80**, 1 (1999).
(23) Y. Qiu and K. Park, *Adv. Drug Deliver. Rev.*, **53**, 321 (2001).
(24) A. Kotal, T. K. Mandal, and D. R. Walt, *J. Polym. Sci. Part A: Polym. Chem.*, **43**, 3631 (2005).
(25) J. H. Kim and T. R. Lee, *Intl. Conf. on Biomedical and Pharmaceutical Engineering 2006 (ICBPE 2006)*, p. 271-275.